

Field theory for magnetic and lattice structure properties of $\text{Fe}_{1+y}\text{Te}_{1-x}\text{Se}_x$

Cenke Xu

Department of Physics, Harvard University, Cambridge MA 02138, USA

Jiangping Hu

Department of Physics, Purdue University, West Lafayette, Indiana 47907, USA

(Dated: April 2, 2024)

We study the magnetism and lattice distortion of $\text{Fe}_{1+y}\text{Te}_{1-x}\text{Se}_x$ with a general field theory formalism, motivated by recent neutron scattering experiments. Besides the Ising nematic order parameter which can be naturally defined in the 1111 and 122 materials, We show that the collinear order observed in Fe_{1+y}Te materials is stabilized by an extra Ising order parameter which doubles the generalized unit cell of the system. By tuning this Ising order parameter, one can drive a transition between collinear and noncollinear spin density wave orders, both of which are observed in the FeTe family. The nature of the quantum and classical phase transitions are also studied in this field theory formalism, with lattice strain tensor fluctuation considered.

The Iron-superconductor, for its potential to shed new light on the non-BCS type of superconductors, has attracted enormous interests since early last year. So far most studies have been focused on the 1111 materials and 122 materials. The 1111 materials have chemical formula LnFeAsO , and Ln represents one of the lanthanides; The 122 materials have chemical formula MFe_2As_2 , and M usually represents one of the alkaline earths. At low temperature, it is confirmed that both 1111 and 122 materials develop $(\pi, 0)$ spin density wave (SDW) [1, 2, 3, 4, 5, 6, 7]. Ever since its discovery, the SDW in 1111 and 122 materials raised a debate about whether this phenomenon should be described by an itinerant electron picture with nesting fermi surface, or a local moment Heisenberg model. This debate is partly due to the fact that the ordering wave vector $(\pi, 0)$ connects two pieces of nearly parallel fermi surfaces, and relatively small magnetic order moment of 1111 materials. However, in the relatively less extensively studied 11 material FeTe family, the answer seems to be more clear, as the order wave vector of these materials is exactly or close to (π, π) [11, 12], which is far away from the nesting wave vector according to LDA calculation [22]. Also, the magnetic order moment can be as large as $2 \mu_B$ [11], which can be naturally understood in terms of local moment picture.

In the low temperature phase of Fe_{1+y}Te , besides the spin density wave (SDW) with wave vector (π, π) , a monoclinic lattice distortion [11] has also been identified. By increasing the excess of Fe in this system, the magnetic order becomes incommensurate [12], with order wave vector deviates from but still close to (π, π) . Also, by replacing Te with Se, both SDW and lattice distortion are suppressed. In Ref. [9], the authors used a local moment Heisenberg model with the nearest, 2nd nearest and 3rd nearest neighbor (J_1 , J_2 , J_3) interactions on the square lattice to describe this system. This simple model captures the correct phases observed experimentally and is also supported by results from LDA calculations[10]. But a model independent general field theory formalism is also necessary, in order to for instance explore the physics beyond the Heisenberg model, and to study the nature of the phase transitions. In this work we will systematically study the Ginzburg-Landau field theory for the

magnetism and lattice structures of FeTe compound and its relative $\text{Fe}_{1+y}\text{Te}_{1-x}\text{Se}_x$.

A general Ginzburg-Landau-Hertz-Millis theory for the 1111 and 122 materials was studied in Ref. [17]. Motivated by experimental facts, it was proposed in Ref. [14, 16] that the true magnetic order in 1111 materials (say LaFeAsO) is developed through two separate steps: first an anisotropic antiferromagnetic (AF) correlation is developed at a relatively higher temperature, and then the long range spin density wave (SDW) order is developed at lower temperature. The anisotropic AF correlation described by an Ising order parameter breaks the reflection symmetry of the lattice along the axis $x = y$, and leads to a tetragonal-orthorhombic lattice distortion. More specifically, this Ising order parameter can be defined as $\tilde{n}_1, \tilde{n}_2, \tilde{n}_3$ and \tilde{n}_4 are Neel order parameters on two sublattices of the square lattice.

In the FeTe family, the SDW and lattice distortion are more complicated, and presumably the anisotropic AF correlations can also develop before the true long range SDW. The SDW order pattern contains four Neel orders on four sublattices [11] (Fig. 1), \tilde{n}_a with $a = 1 \sim 4$. Two Ising order parameters which obviously break the lattice reflection symmetry are \tilde{n}_1, \tilde{n}_3 and \tilde{n}_2, \tilde{n}_4 . \tilde{n}_1 and \tilde{n}_2 can develop long range order before \tilde{n}_a does, and the symmetry of \tilde{n}_i enables them to distort the lattice from tetragonal to monoclinic once they develop long range order. However, \tilde{n}_1 and \tilde{n}_2 are not independent Ising order parameters in the free energy there should be a term which breaks the degeneracy between $\tilde{n}_1, \tilde{n}_2 > 0$ and $\tilde{n}_1, \tilde{n}_2 < 0$. Later on we will show in the ground state $\tilde{n}_1, \tilde{n}_2 < 0$, and the energy barrier between states with $\tilde{n}_1, \tilde{n}_2 < 0$ and $\tilde{n}_1, \tilde{n}_2 > 0$ is estimated to be about $J_1^2 = J_3$ for the J_1, J_2, J_3 model.

Let us first study the structure transitions, and tentatively ignore the magnetic orders. In the high temperature symmetric phase, the Fe-Te plane enjoys the following symmetries: $P_z, T_x, P_z, T_y, P_z, P_x, P_z, P_y, P_z$ and P_x are reflections $\hat{z} \rightarrow -\hat{z}$ and $\hat{x} \rightarrow -\hat{x}$ with origin located on one of the Fe atoms, T_x and T_y are translations. Although the true unit cell of the Fe-Te plane always involves two Fe atoms, one can define a one Fe unit cell based on the generalized translations

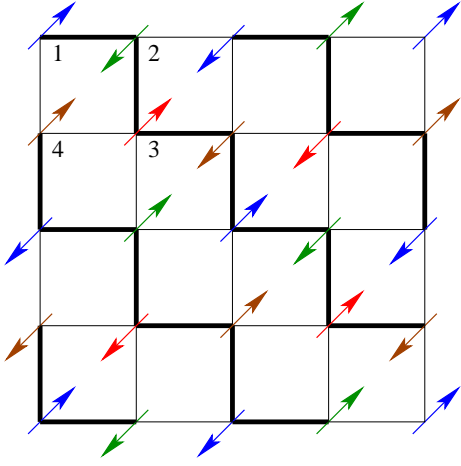


FIG. 1: The collinear magnetic order of FeTe family. The four sublattices form Neel orders separately, and the thick lines represent links with stronger AF correlations, which doubles the unit cell defined by generalized translation operators T_x^0 and T_y^0 . It is possible that the anisotropic AF correlations develop long range order before the actual SDW pattern.

$T_x^0 = P_z T_x$ and $T_y^0 = P_z T_y$, and we will use this generalized unit cell hereafter. The lattice distortion observed in experiments[11] breaks all of the symmetries including T_x^0 and T_y^0 . The lattice distortion favors the antiferromagnetic correlations along the zig-zag stripes, and there are in total 4 different degenerate zig-zag configurations. We can describe these zig-zag AF correlation stripes with two Ising order parameters ϕ_1 and ϕ_2 . $\phi_1 = 1$ represents two degenerate zig-zag correlation stripe patterns along the $x = y$ direction, and $\phi_2 = 1$ represents two zig-zag correlation stripes along the $x = -y$ direction. One can write down a Ginzburg-Landau free energy for the coarse-grained modes of ϕ_a according to the symmetry of the system:

$$F = \sum_{a=1}^2 \left[(r_a \phi_a)^2 + r_1 \phi_a^2 + u_0 \phi_a^4 + u_2 \phi_1^2 \phi_2^2 + O(\phi^6) \right] \quad (1)$$

Here we need $u_2 > 2u_0$ to make sure that in the ordered phase $\phi_1 \phi_2 \neq 0$, which is the case in the real system.

Another more intuitive way to describe the ϕ_a variables, is to introduce complex field $\psi = \phi_1 + i\phi_2$, and the free energy Eq. 1 can be rewritten as

$$F = \sum_{a=1}^2 \left[r_a \phi_a^2 + r_1 \phi_a^2 + g_1 \phi_a^4 + g_4 (\phi_a^4 + \phi_a^{*4}) + O(\phi^6) \right] \quad (2)$$

The free energy up to the forth order of ϕ_a and ψ enjoys an enlarged Z_4 symmetry, which can be viewed as an Z_4 anisotropy of an XY or U(1) quantity. It is well-known that the Z_4 anisotropy at the 3D XY transition is irrelevant [19], so our first conclusion is that, in the most simplified situation the finite temperature transition of ϕ_a is a 3D XY transition. In Eq. 1 and Eq. 2 The terms at the 6th order or higher will break this Z_4 symmetry, however, those terms will also be irrelevant at the 3D XY transition, so we will ignore them from now on.

According to the symmetry, the Ising fields ϕ_1 and ϕ_2 couple to the Ising field $\phi_1 \phi_2$ in the following manner:

$$F = f + \left(\frac{r_1}{2} \phi_1^2 + \frac{r_2}{2} \phi_2^2 \right) \quad (3)$$

The Ising field $\phi_1 \phi_2$ describes the anisotropic AF correlation which breaks no translational symmetry, but breaks the reflection symmetries $P_z = P_x$ and $P_z = P_y$. The full free energy reads:

$$F = \sum_{a=1}^2 \left[(r_a \phi_a)^2 + r_1 \phi_a^2 + (r_2 \phi_a)^2 + r_2 \phi_a^2 + f + \left(\frac{r_1}{2} \phi_1^2 + \frac{r_2}{2} \phi_2^2 \right) + \dots \right] \quad (4)$$

The ellipses include all the quartic terms. Both r_1 and r_2 are tuned by temperature. By minimizing Eq. 4, one can obtain the mean field global phase diagram plotted against $r = r_1 + r_2$ and $r = r_1 - r_2$ (Fig. 2a). There are in total three different regions: **1**), when $r_1 > r_2$, there are two transitions, with one Ising transition for ϕ_1 and another Ising transition for one of the ϕ_a , since in this region ϕ_1 has a much stronger tendency to order compared with ϕ_a ; **2**), when $r_1 = r_2$, there is an intermediate region with first order transition, and ϕ_1 and ϕ_a will order at the same temperature. The first order nature of this transition is due to the cubic coupling term $F = f + \dots$; **3**), when $r_1 < r_2$ there is still one single transition, but this transition is second order. This transition can be studied by integrating out ϕ_a from free energy Eq. 4, and the resultant free energy for ϕ_1 is the same as Eq. 2, which describes a 3D XY transition as was discussed previously.

So far we have ignored the lattice elasticity, which will potentially change the nature of the transitions discussed above [17]. In region **1**) discussed in the previous paragraph, the Ising field $\phi_1 \phi_2$ will couple to the uniaxial shear strain field of the lattice:

$$F = f + \left(\frac{r_1}{2} \phi_1^2 + \frac{r_2}{2} \phi_2^2 \right) + \dots \quad (5)$$

\mathbf{u} represents the local displacement vector of the lattice. By integrating out the displacement vector \mathbf{u} , we can show that the fluctuation of the displacement vector \mathbf{u} will increase the effective spatial dimension at the transition of $\phi_1 \phi_2$, and drive the transition of $\phi_1 \phi_2$ mean field like, as was studied carefully in Ref. [17]. At the mean field transition the specific heat curve will have a discontinuity instead of a peak, as was observed in electron-doped 122 materials [8]. Unlike the field $\phi_1 \phi_2$, in region **1**) the field ϕ_a that breaks the translational symmetry will only couple to the bulk strain field in the following way:

$$F = f + \sum_{a=1}^2 \left[r_a \phi_a^2 + r_1 \phi_a^2 + r_2 \phi_a^2 + r_3 \phi_a^2 \right] \quad (6)$$

We can estimate the scaling dimension of the coupling constant f_{μ} as the following: The scaling dimension of ϕ_a^2 at the 3D Ising transition is $[\phi_a^2] = 3 - 1 = 2$, and the scaling dimension of displacement vector \mathbf{u} is $[\mathbf{u}] = 1 - 2 = -1$. Therefore the dimension of f_{μ} is $[f_{\mu}] = 3 - 2 + 1 = 2$.

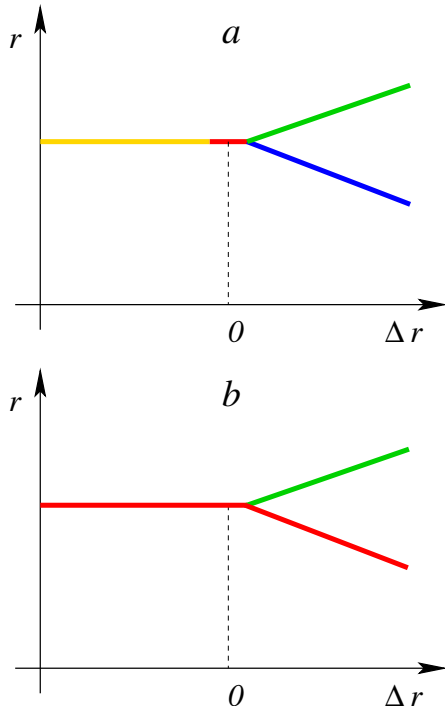


FIG. 2: The global phase diagrams for Eq. 4 and Eq. 10 plotted against $r = r_1 + r_2$, and $r = r_1 - r_2$. For Eq. 4, Fig. a represents the case without considering lattice elasticity. In this case the red line is a first order transition; the golden line is a 3D XY Wilson-Fisher transition; the green line and blue line are 3D Ising transitions for \tilde{a} and \tilde{a} respectively. For Eq. 4, Fig. b represents the phase diagram with coupling to the lattice strain tensor, the 3D XY transition and the 3D Ising transition of \tilde{a} become first order, the 3D Ising transition of \tilde{a} becomes a mean field transition. For Eq. 10, Fig. a and Fig. b represent the case without and with considering itinerant electron particle-hole excitations respectively. If a two dimensional model is taken, the nature of the transitions is almost the same as Eq. 4.

$\text{ising} = 2 > 0$. So this coupling will lead to a relevant perturbation at the 3D Ising transition of \tilde{a} . This relevant perturbation will likely drive the transition first order [21]. This argument of scaling dimension is essentially the same as the well-known Harris criterion in the disordered system.

In region 3), as was shown before, after integrating out \tilde{a} , the transition is described free energy Eq. 2, which describes a 3D XY transition. The 3D XY transition is also affected by the lattice elasticity. First of all, \tilde{a} is also coupled to the bulk strain field $F_{\mu\nu} = \frac{1}{2}(\epsilon_x u_x + \epsilon_y u_y + \epsilon_z u_z)$, because $\epsilon_{xy} = 2\epsilon_{yx} < 0$ this coupling will not introduce any relevant perturbations. However, $\epsilon_{12}^2 \in \mathbb{R} \in [2]$ will couple to the shear strain field $\epsilon_{xx} u_x - \epsilon_{yy} u_y$. To check whether this coupling is relevant or not, we just need to compare the scaling dimension of ϵ_{12}^2 to $D=2$ at the three dimensional XY transition. At the 3D XY critical point, the scaling dimension $[\epsilon_{12}^2] = 1.234 < 3=2$ [19], hence this coupling will indeed generate relevant perturbation at the 3D XY transition, which likely drives the transition a first order one. Therefore after considering the lattice elasticity, the global phase dia-

gram is modified to Fig. 2b

Now let us consider the SDW order, described by four Neel order parameters \tilde{a}_a with $a = 1 \sim 4$, and let us ignore the Ising fields \tilde{a}_a first. Besides the ordinary kinetic terms in the free energy, several linear spatial derivative terms are also allowed by the symmetry of the system, therefore a most general free energy for the Neel order parameter \tilde{a}_a reads:

$$F_{\tilde{a}} = \sum_{a=1}^4 J_3 (r - \tilde{a}_a)^2 + \tilde{g}_1 \tilde{a}_1 \tilde{a}_2 + \tilde{g}_4 \tilde{a}_4 \tilde{a}_3 + \tilde{g}_2 \tilde{a}_2 \tilde{a}_3 + \tilde{g}_3 \tilde{a}_3 \tilde{a}_4 : \quad (7)$$

The \hat{z} direction dispersion has been ignored. This theory can also be viewed as a low energy field theory for the lattice $J_1 J_2 J_3$ Heisenberg model, with J_1 , and $g = J_2^2 = J_3$. If $J_1 J_2 < 0$, An infinitesimal J_1 inevitably drives the system to an incommensurate order, with ordering wave vector $\vec{Q} = (\pi/2 + q; \pi/2 - q)$, $q = J_3/J_1$. However, if $J_1 J_2 > 0$, the minima of the dispersion remains at $\vec{Q} = (\pi/2; \pi/2)$ for small enough J_1 . The energy difference between the two states with $J_1 J_2 < 0$ and $J_1 J_2 > 0$ is about $J_1^2 = J_3$, or in other words there is an effective coupling $J_1 J_2$ in the free energy, which is proportional to $J_1^2 = J_3$.

In the phase with $J_1 J_2 < 0$ The collinear commensurate order is stabilized by coupling the SDW order parameter to the Ising fields \tilde{a}_a . Again, the symmetry of the system allows the following coupling:

$$F_{\tilde{a}} = \tilde{g}_1 (\tilde{a}_1 \tilde{a}_2 + \tilde{a}_2 \tilde{a}_3 + \tilde{a}_3 \tilde{a}_4 + \tilde{a}_4 \tilde{a}_1) + \tilde{g}_2 (\tilde{a}_1 \tilde{a}_2 - \tilde{a}_2 \tilde{a}_3 + \tilde{a}_3 \tilde{a}_4 - \tilde{a}_4 \tilde{a}_1) : \quad (8)$$

After diagonalizing the quadratic part of the entire free energy (Eq. 8), we can see that if $J_1 > 0$ and $J_2 < 0$ the system favors $\tilde{a}_2 \neq 0$ while $\tilde{a}_1 = 0$. Therefore there is indeed an effective coupling $F_{\tilde{a}}$, as Eq. 3.

Whether the system develops incommensurate or commensurate order, depends on the competition between the terms with linear spatial derivatives, and the terms with coupling to \tilde{a}_a . When \tilde{a}_a dominates $J_1^2 = J_3$, the commensurate collinear order is stabilized, otherwise the system develops the incommensurate coplanar order. Assuming $J_1 = J_1 > 0$, and hence at low temperature \tilde{a}_2 orders while \tilde{a}_1 remains disordered, a transition between incommensurate and commensurate orders can be driven by tuning $J_1 = \tilde{a}_2$. Experimentally this transition can be achieved by changing the excess of Fe [12]. If we diagonalize the quadratic part of the SDW free energy, the mode with the lowest minimum takes the following form:

$$E(\vec{q}) = g_1 \tilde{a}_1 + g_2 \tilde{a}_2 + g_3 (\alpha_x^2 + \alpha_y^2) \frac{q_x^2 + q_y^2}{2} + g_4 (\alpha_x - \alpha_y)^2 : \quad (9)$$

One can check that by tuning J_1 , there is a transition between commensurate and incommensurate order, and the incommensurate wave vector is a continuous function of J_1 . The commensurate collinear SDW order has ground state manifold S^2

times lattice transformation degeneracy, while the incommensurate coplanar SDW order has ground state manifold $S^3=Z_2$. The transition between these two phases can be viewed as condensation of an U(1) degree of freedom [18], because the manifold S^3 is locally $S^2 \times S^1$. However, as was shown in Ref. [18], the condensation of this U(1) degree of freedom does not belong to the XY universality class, because the spin-wave fluctuation of the collinear SDW order parameter at the transition will again effectively increase the spatial dimension of the XY transition, therefore the collinear/coplanar phase transition always belongs to the mean field universality class, for both 3D classical and 2+1d quantum cases [18].

It is also interesting to study the quantum phase transitions of ϕ_a and ϕ_b at zero temperature, and we will take a simple two dimensional model to emphasize the physics within the Fe-Te plane, and also partly motivated by the fact that the band structure calculated by LDA has a much weaker z direction dispersion for FeTe and FeSe compared with the 122 compounds [22]. The Lagrangian describing the quantum phase transitions is very similar to the free energy Eq. 4:

$$\begin{aligned} L = & \sum_{a=1}^2 \left(\dot{\phi}_a^2 + v^2 q^2 + r_1 \right) \phi_a^\dagger \phi_a + \\ & + \left(\dot{\phi}_b^2 + v^2 q^2 + r_2 \right) \phi_b^\dagger \phi_b + \\ & + f; \quad \left(\frac{1}{2} \phi_a^2 + \frac{1}{2} \phi_b^2 \right) + \end{aligned}$$

The phase diagram is actually quite similar to Fig. 2, with r tuned by replacing Te with Se in $Fe_{1-y}Te$, as shown experimentally [11, 12]. Phase diagram Fig. 2a corresponds to the case without fermi pockets, or phase transitions in a superconductor with fully gapped fermi surface, and the nature of the phase transitions described by Eq. 10 is the same as the phase transitions in Eq. 4.

The fermi surface of the 11 materials have been observed by ARPES [23], and the structure qualitatively agrees with the LDA calculation. If the fermi surfaces are not gapped, the coupling between the bosonic order parameters ϕ_a and ϕ_b with the particle-hole excitations around the fermi surface will change the nature of the quantum phase transitions, or more specifically change the dynamical exponent z . Phase diagram Fig. 2b corresponds to the case with ungapped fermi pockets. The green line becomes a $z = 3$ quantum phase transition, as discussed in Ref. [16, 20], because the order ϕ_a carries zero momentum, and the particle-hole excitation around the fermi surface will induce a decay term of ϕ_a^2 :

$$L_{\text{red}} = \sum_{\mathbf{q}} \left(\dot{\phi}_a^2 + v^2 q^2 + r_1 \right) \phi_a^\dagger \phi_a + \frac{1}{q} \phi_a^2 \phi_b^\dagger \phi_b + \dots \quad (11)$$

A similar decay term does not exist at the quadratic level in the Lagrangian of ϕ_b , because ϕ_b carries momentum ($\mathbf{q} = 2\mathbf{k}; \mathbf{q} = 2\mathbf{k}$). Based on the LDA calculation [22] and also ARPES measurements [23], the momentum ($\mathbf{q} = 2\mathbf{k}; \mathbf{q} = 2\mathbf{k}$) does not connect two pieces of the fermi surfaces. However, the particle-hole excitation can also modify the quartic terms of the Lagrangian Eq.

10. The coupling between ϕ_a^2 and fermion density will lead to a term

$$L_{\text{red}} = \sum_{\mathbf{q}} \left(\dot{\phi}_a^2 + v^2 q^2 + r_1 \right) \phi_a^\dagger \phi_a + \frac{1}{q} \phi_a^2 \phi_b^\dagger \phi_b + \dots \quad (12)$$

which is a relevant perturbation at the 3D Ising transition due to the positive γ_{Ising} . On the left side of Fig. 2b with $r < 0$, the transition was a 3D XY transition without fermi pockets. The Fermi pockets will generate a term $\text{Re}[\phi_a^2] \frac{1}{q} \text{Re}[\phi_b^2]$, which is again relevant at the 3D XY transition. Therefore the red line in Fig. 2b is a first order transition for a 2 dimensional quantum model.

In summary, we have shown that $Fe_{1-y}Te$ materials are characterized by two Ising order parameters: one Ising nematic order which has been found in 1111 and 122 materials and the other Ising order which doubles the unit cell of systems. We have also calculated the phase diagram and the nature of phase transitions. Unlike long-range SDW orders which are easily destroyed by replacing Te with Se in $FeTe_{1-x}Se_x$, the Ising orders may survive in larger doping regions [14, 16] and coexist with superconducting states. Experimentally, it is possible to detect the Ising orders from their broken symmetries, for example, using polarized light in angle resolved photoemission spectra.

Acknowledge We thank B.A. Bernevig for useful discussions. JPH is supported by the NSF under grant No. PHY-0603759.

-
- [1] Clarina de la Cruz, Q. Huang, J. W. Lynn, Jiying Li, W. Ratcliff II, J. L. Zarestky, H. A. Mook, G. F. Chen, J. L. Luo, N. L. Wang, Pengcheng Dai, *Nature* **453**, 899 (2008).
 - [2] M. A. McGuire, A. D. Christianson, A. S. Sefat, B. C. Sales, M. D. Lumsden, R. Jin, E. A. Payzant, D. Mandrus, Y. Luan, V. Keppens, V. Varadarajan, J. W. Brill, R. P. Hermann, M. T. Sougrati, F. Grandjean, G. J. Long, *Phys. Rev.* **78**, 094517 (2008).
 - [3] Q. Huang, Y. Qiu, Wei Bao, J.W. Lynn, M.A. Green, Y. Chen, T. Wu, G. Wu, X.H. Chen, *arXiv:0806.2776* (2008).
 - [4] C. Krellner, N. Caroca-Canales, A. Jesche, H. Rosner, A. Ormeci, C. Geibel, *Phys. Rev. B* **78**, 100504(R) (2008).
 - [5] J.-Q. Yan, A. Kreyssig, S. Nandi, N. Ni, S. L. Bud'ko, A. Kracher, R. J. McQueeney, R. W. McCallum, T. A. Lograsso, A. I. Goldman, P. C. Canfield, *Phys. Rev. B* **78**, 024516 (2008).
 - [6] Jun Zhao, W. Ratcliff II, J. W. Lynn, G. F. Chen, J. L. Luo, N. L. Wang, Jiangping Hu, Pengcheng Dai, *Phys. Rev. B* **78**, 140504(R) (2008).
 - [7] A.I. Goldman, D.N. Argyriou, B. Ouladdiaf, T. Chatterji, A. Kreyssig, S. Nandi, N. Ni, S. L. Bud'ko, P.C. Canfield, R. J. McQueeney, *Phys. Rev. B* **78**, 100506(R) (2008).
 - [8] Jiun-Haw Chu, James G. Analytis, Chris Kucharczyk, Ian R. Fisher, *arXiv:0811.2463* (2008).
 - [9] Chen Fang, B. Andrei Bernevig, Jiangping Hu, *arXiv:0811.1294* (2008).
 - [10] Fengjie Ma, Wei Ji, Jiangping Hu, Zhong-Yi Lu and Tao Xiang, *arXiv:0809.4732* (2008).
 - [11] Shiliang Li, Clarina de la Cruz, Q. Huang, Y. Chen, J. W. Lynn, Jiangping Hu, Yi-Lin Huang, Fong-chi Hsu, Kuo-Wei

- Yeh, Maw-Kuen Wu, Pengcheng Dai, Phys. Rev. B 79, 054503 (2009).
- [12] Wei Bao, Y. Qiu, Q. Huang, M.A. Green, P. Zajdel, M.R. Fitzsimmons, M. Zhernenkov, M. Fang, B. Qian, E.K. Vehstedt, J. Yang, H.M. Pham, L. Spinu, Z.Q. Mao, arXiv:0809.2058 (2008).
- [19] Pasquale Calabrese, Andrea Pelissetto, Ettore Vicari, cond-mat/0306273, (2003).
- [14] Chen Fang, Hong Yao, Wei-Feng Tsai, JiangPing Hu, Steven A. Kivelson, Phys. Rev. B 77, 224509 (2008).
- [15] P. Chandra, P. Coleman, and A. I. Larkin, Phys. Rev. Lett 64, 88 (1990).
- [16] Cenke Xu, Markus Mueller, Subir Sachdev, Phys. Rev. B 78, 020501(R) (2008).
- [17] Yang Qi and Cenke Xu, arXiv:0812.0016 (2008).
- [18] Cenke Xu and Subir Sachdev, Phys. Rev. B 79, 064405 (2009).
- [19] Pasquale Calabrese, Andrea Pelissetto, Ettore Vicari, cond-mat/0306273, (2003).
- [20] Vadim Oganesyan, Steven Kivelson, Eduardo Fradkin, Phys. Rev. B 64, 195109 (2001).
- [21] D. Bergman and B. I. Halperin, Phys. Rev. B. **13**, 2145 (1976).
- [22] Alaska Subedi, Lijun Zhang, David J. Singh, Mao-Hua Du, Phys. Rev. B 78, 134514 (2008).
- [23] Y. Xia, D. Qian, L. Wray, D. Hsieh, G.F. Chen, J.L. Luo, N.L. Wang, M.Z. Hasan, arXiv:0901.1299 (2009).